

SCIENTIFIC REPORTS



OPEN

High-throughput optimisation of light-driven microalgae biotechnologies

Shwetha Sivakaminathan, Ben Hankamer , Juliane Wolf & Jennifer Yarnold 

Microalgae biotechnologies are rapidly developing into new commercial settings. Several high value products already exist on the market, and systems development is focused on cost reduction to open up future economic opportunities for *food, fuel* and *freshwater* production. Light is a key environmental driver for photosynthesis and optimising light capture is therefore critical for low cost, high efficiency systems. Here a novel high-throughput screen that simulates fluctuating light regimes in mass cultures is presented. The data was used to model photosynthetic efficiency (PE_{μ} , mol photon⁻¹ m²) and chlorophyll fluorescence of two green algae, *Chlamydomonas reinhardtii* and *Chlorella* sp. Response surface methodology defined the effect of three key variables: *density factor* (D_f , 'culture density'), *cycle time* (t_c , 'mixing rate'), and *maximum incident irradiance* (I_{max}). Both species exhibited a large rise in PE_{μ} with decreasing I_{max} and a minimal effect of t_c (between 3–20 s). However, the optimal D_f of 0.4 for *Chlamydomonas* and 0.8 for *Chlorella* suggested strong preferences for dilute and dense cultures respectively. *Chlorella* had a two-fold higher optimised PE_{μ} than *Chlamydomonas*, despite its higher light sensitivity. These results demonstrate species-specific light preferences within the green algae clade. Our high-throughput screen enables rapid strain selection and process optimisation.

Green algae are oxygenic photosynthetic organisms which, like higher plants and cyanobacteria, have evolved over 3 billion years to tap into the huge energy resource of the sun. This energy is used to fix CO₂, releasing O₂ as a by-product and producing biomass rich in proteins, lipids, starch, bioactive compounds and phytonutrients. Consequently, single celled green algae (microalgae) are increasingly being integrated into industrial production systems to realise solar driven biotechnologies. Microalgae technologies are already being exploited commercially to produce high value commodities (e.g. functional foods, feeds, protein therapeutics and chemicals)^{1–3} and the knowledge gained is driving down production costs toward the levels required to expand low value market opportunities including fuels and fertilisers as well as ecosystem services (e.g. water treatment and CO₂ sequestration)^{4–6}. The first step of all solar driven microalgae processes is light capture and conversion to chemical energy (ATP, NADPH), and the optimisation of this step is therefore essential to develop high-efficiency economic solutions^{7–9}. In outdoor mass cultures, the light reaching the surface of the pond or bioreactor is highly variable over the day, ranging from light limiting during early/late hours of the day or periods of high cloud cover, to photo-inhibiting conditions (up to 2,000 μmol m⁻² s⁻¹) during mid-day in locations receiving high solar radiation. Within the culture itself, cells are exposed to high light gradients as they cycle from the illuminated surface (often inhibitory light levels) to deep within the culture (light limiting or dark conditions). This fluctuating light regime within the mass culture is governed by the optical properties of the culture (based on cell size, cell number and pigment content) while the frequency with which cells cycle between the light and dark zones is regulated by mixing rate as well as the photobioreactor geometry which influences the light distribution through the optical pathlength and the surface to volume ratio. The relatively rapid light fluctuations within the culture affect the photo-regulatory response, while the relatively slow environmental light fluxes affect photoacclimation, both leading to changes in the overall productivity of the culture^{10–12}.

Defining and optimising the effects and interactions of the variables that govern a given light regime is a challenge that requires comparatively large experimental datasets which can be laborious and expensive to obtain using traditional pilot- or even laboratory-scale bioreactors. The high-throughput light screen method presented here has been designed to simulate light regimes encountered in mass cultured photobioreactors under 'typical'

The University of Queensland, Institute for Molecular Bioscience, 306 Carmody Road, St Lucia, Australia. Correspondence and requests for materials should be addressed to J.W. (email: j.wolf@imb.uq.edu.au) or J.Y. (email: j.yarnold@imb.uq.edu.au)

outdoor production conditions to enable process optimisation, model guided system design, species selection and a better extrapolation of laboratory results to field trials.

The light screen collected data from LED illuminated microwells, and Response Surface Methodology was employed to predictively model photosynthetic efficiency (PE_{μ}), to define both main effects and the pair-wise interactions between the light factors that govern it and to identify the conditions that yield optimum productivity. As fluctuating light can effect photoregulation and photoacclimation, we also investigated some of these underlying mechanisms to assess the extent of their effect on PE_{μ} .

A full factorial experimental design was employed, with quadratic models fitted to the data to measure the PE_{μ} in response to variations of three key factors that govern the light regime to which cells in mass culture are exposed: density factor (D_f , -), defined as the proportion of the time that cells are in the dark zone (t_{dark} , s) compared with the total time in both light (t_{light} , s) and dark zones; cycle time (t_c , s), which is defined by the mixing rate, or the total time of a cell's fluctuation between light and dark zones for one cycle along the culture depth; and maximum irradiance (I_{max} , $\mu\text{mol photons m}^{-2} \text{s}^{-1}$) defined as the irradiance entering the photobioreactor at the illuminated surface (Fig. 1A). Dark was defined as $<5 \mu\text{mol PAR}$ at which respiration typically exceeds photosynthesis (the compensation point)^{13,14}. The three factors (D_f , t_c , I_{max}) affect the average irradiance (I_{avg}), which is the integration of light experienced by the cells over the entire light cycle (Fig. 1B). Our miniaturised and automated screen enables the analysis of the interactions between the three light-dependent factors and generates a strain-specific model that can be used to optimise production conditions or predict productivities for different production scenarios.

This empirical model is an alternative approach to traditional models based on photosynthetic irradiance (P-I) curves. It only requires knowledge of the density factor, incident irradiance and mixing rate. The D_f for a given species and reactor geometry can be easily found (indoor or outdoor) for a given incident irradiance by measuring the depth of culture at the point where light is reduced to $<5 \mu\text{mol m}^{-2} \text{s}^{-1}$ (i.e. start of the “dark zone”) and calculating the ratio of this depth to the total culture depth (usually fixed). This can be correlated to a range of optical densities (or biomass dry weights) to provide a simple method to establish what D_f a reactor will have at a known culture density, pathlength and incident irradiance. Since D_f has been determined as a critical factor in this and other studies, we believe that this is another useful modelling tool for process design.

Two biotechnologically relevant microalgae strains were analysed in this study: *Chlamydomonas reinhardtii* (*Chlamydomonas*), the model alga most used in photosynthetic studies^{15,16} and for heterologous protein expression^{17,18}, and a strain of *Chlorella* sp, 11_H5 (*Chlorella*) isolated in Australia which was found to have high biomass productivity at laboratory and pilot scale^{19,20}. *Chlamydomonas* (originally isolated from soil)²¹ has successfully transitioned from land to water in laboratory conditions, arguably owing to its robust and evolved photosynthetic machinery that protects it from oxidative stress and changing environmental conditions²². Hence, understanding the interplay between photosynthetic regulation, photoacclimation and its effect on growth and biomass productivity would determine the feasibility of delivering functional microalgae biotechnologies. This paper presents a high-throughput miniaturised light optimisation screen (allowing up to 18 different combinations of light regime and up to 1,728 conditions), designed to identify species-specific illumination conditions that maximise photosynthetic efficiency and productivity to fast track systems optimisation.

Results

High-throughput screen (HTS) of simulated light regimes in mass cultures. To analyse the effects of varying levels of I_{max} , D_f and t_c (Fig. 1B) on the PE_{μ} of microalgae, light simulations were performed on dilute 150 μl microwell cultures (5 mm pathlength)²³, each illuminated using individual LEDs (Fig. 1C). The intensity of photosynthetically active radiation (400–700 nm, PAR) emitted by the LEDs was programmed (Arduino® integrated circuit and controller) to mimic a sinusoidal trajectory of a cell cycling in a one-dimensionally illuminated culture (i.e. an open pond) between the illuminated surface and the dark zone (Fig. 1B)¹⁰. In this way, the light regime encountered by the incubated cells in each well was a function of the LED's illumination profile, thereby allowing tight control of the levels of each factor (I_{max} , D_f and t_c), (Fig. 1A). A robotic arm was programmed to take the plates to a reader at determined time intervals where rapid measurements of optical density and fluorescence can be taken. Here, two strains were analysed for the initial HTS light simulations, however, this method can rapidly be used to model up to 32 strains run in triplicate in one experiment.

Figure 1A depicts the three levels of each factor (I_{max} , D_f , t_c) and the real-world phenomena they represent based on information from literature^{24–26} and on experimental data^{27–29}. A low (0.2) or high (0.8) D_f represents a low or high cell/biomass density respectively (e.g. dilute cultures at the beginning of cultivation versus dense cultures at harvest in a batch production regime). The system is able to analyse any range between 10 ms fluctuations to constant light. The cycle time of 3–20 s represents typical ‘mixing’ cell cycle rates through the optical pathlength of photobioreactors, where a t_c of 3, 10, and 20 s represents rapid, moderate or slow mixing, as might occur in a tubular PBR, thick flat panel PBR and open pond respectively. The t_c is influenced by mixing and/or sparging rates, reactor pathlength, or a combination of the two, which can vary for individual reactors depending on cultivation regime. The I_{max} values represent the incident solar radiation in the early morning and late afternoon ($375 \mu\text{mol m}^{-2} \text{s}^{-1}$), mid-morning and -afternoon ($750 \mu\text{mol m}^{-2} \text{s}^{-1}$), and noon ($1500 \mu\text{mol m}^{-2} \text{s}^{-1}$) respectively. I_{max} values are based on the average annual solar radiation levels for Brisbane, Australia^{30,31}, and are representative of other high solar regions that are suitable for outdoor microalgae production. The simulation of these three factors at three levels each via programmed changes in LED light flux over time are depicted in Fig. 1B. This approach provided a complete factorial design (3^3) of 27 combinations for model fitting of the main response variable, PE_{μ} (Table 1) and underlying responses at the level of PSII (Table 2).

A further dataset with a D_f of 0.6 (at each level of I_{max} and t_c) provided 9 independent data points used for model validation and goodness of fit (Table 1, validation data are indicated by ‘*’. See section (Model validation) shows that the light factors D_f , I_{max} and t_c can be used to predict PE_{μ} accurately in *Chlorella* and moderately in

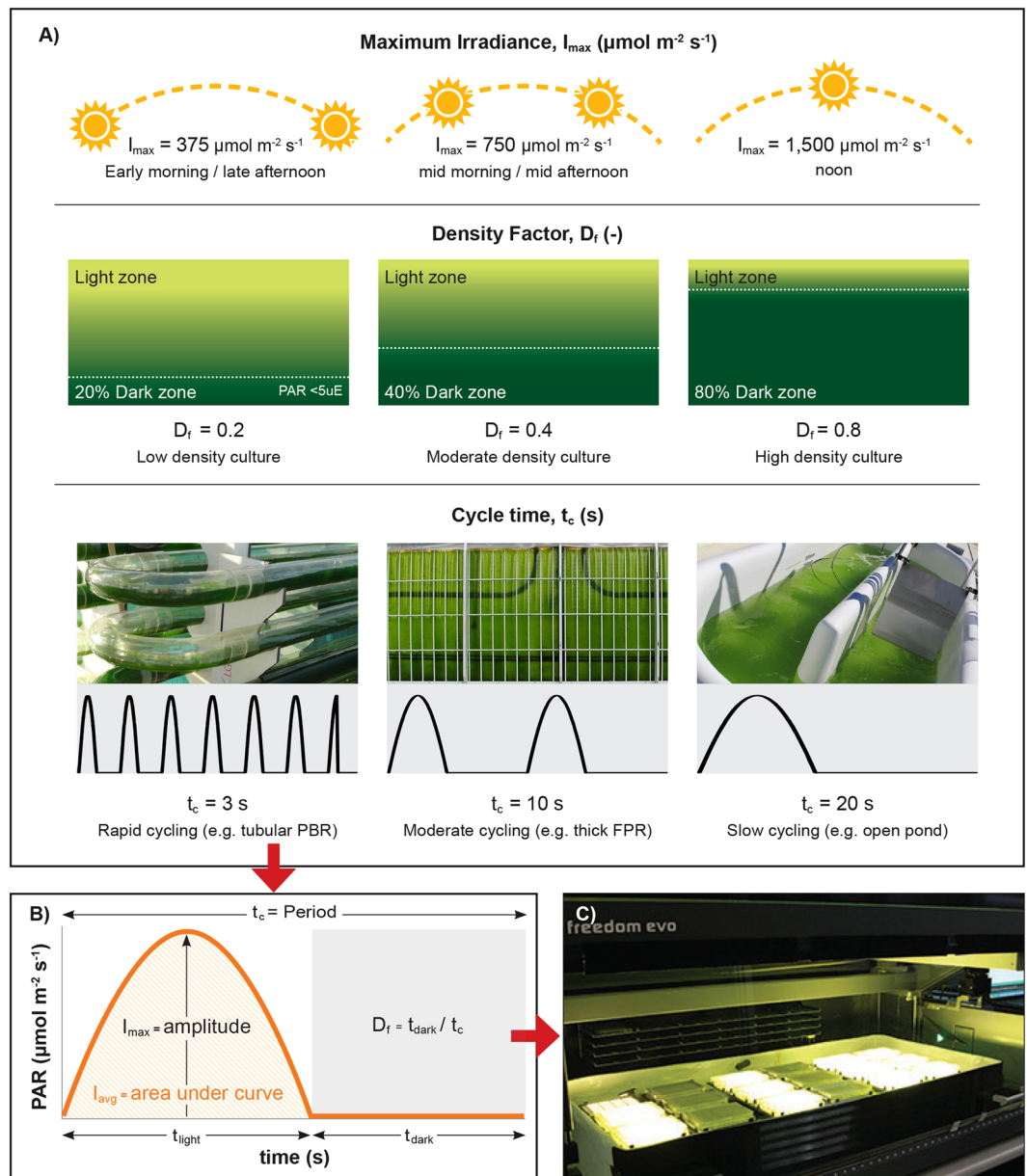


Figure 1. Experimental design for high-throughput light simulations of cells cycling in outdoor microalgae mass cultures. (A) Depicts the 3 factors that affect the light regime experienced by cells cycling in mass cultures: I_{\max} , D_f and t_c , and the levels used for the full factorial experimental design which are based on ‘typical’ outdoor conditions. (B) Each combination of light factors was programmed by changing the light intensity of the LEDs over the cycle time, assuming cell cycling occurs in a sinusoidal trajectory. Here, I_{\max} is the amplitude of the sine, simulating the maximum irradiance that a cell would receive when at the ‘surface’ of a mass culture, D_f is the proportion of time that PAR is below $5 \mu\text{mol m}^{-2} \text{s}^{-1}$ in one period; this simulates the fraction of time that a cell spends in the dark, depending on the culture density, and t_c is the period of one sine wave, that simulates the time required for a cell to cycle through the reactor. I_{avg} is the integration of light received, simulating the average irradiance or light dose received by the cell. Here t_{light} and t_{dark} are the time cells receive PAR ($>5 \mu\text{mol m}^{-2} \text{s}^{-1}$) and no PAR ($<5 \mu\text{mol m}^{-2} \text{s}^{-1}$) respectively. (C) The programmed LEDs form part of an 18-plate microwell robotic system. *Chlamydomonas* and *Chlorella* were incubated in 96-well plates placed on LED arrays with one LED per microwell and one unique light regime per plate. All light regimes occurred over a photoperiod of 16 h day^{-1} and a dark period of 8 h day^{-1} .

Chlamydomonas) for results). For all treatments, the combination of each D_f and I_{\max} also resulted in 12 unique integrated average irradiance levels, I_{avg} ($\text{mol photons m}^{-2} \text{h}^{-1}$). Additional experiments compared the PE_{u} between cells exposed to fluctuating regimes with cells exposed to constant illumination (control) with the same I_{avg} to compare the effect of light regime and light dose (Fig. 2C, Supplementary Table S1, Supplementary Fig. S4).

I_{\max}		D_f		t_c		I_{avg}	PE_{μ} (mol photon $^{-1}$ m 2)	
Actual ($\mu\text{mol m}^{-2} \text{s}^{-1}$)	Coded	Actual (—)	Coded	Actual (s)	Coded	(mol m $^{-2}$ h $^{-1}$)	<i>Chlamydomonas</i>	<i>Chlorella</i>
375	-1	0.2	-1	3	-1.73	0.619	0.118 ± 0.0030	0.136 ± 0.017
				10	0		0.099 ± 0.0093	0.142 ± 0.018
				20	1		0.107 ± 0.0031	0.151 ± 0.026
		0.4	0	3	-1.73	0.490	0.174 ± 0.0070	0.183 ± 0.012
				10	0		0.133 ± 0.0079	0.149 ± 0.001
				20	1		0.094 ± 0.0070	0.132 ± 0.018
		0.6*	—	3	-1.73	0.367	0.088 ± 0.0066	0.176 ± 0.007
				10	0		0.099 ± 0.0010	0.167 ± 0.011
				20	1		0.084 ± 0.0100	0.149 ± 0.007
		0.8	1	3	-1.73	0.18	0.040 ± 0.0028	0.277 ± 0.022
				10	0		0.048 ± 0.0000	0.197 ± 0.014
				20	1		0.047 ± 0.0107	0.159 ± 0.006
750	0	0.2	-1	3	-1.73	1.242	0.078 ± 0.0037	0.039 ± 0.003
				10	0		0.063 ± 0.0013	0.054 ± 0.002
				20	1		0.053 ± 0.0022	0.076 ± 0.001
		0.4	0	3	-1.73	0.979	0.060 ± 0.0121	0.087 ± 0.004
				10	0		0.061 ± 0.0040	0.087 ± 0.006
				20	1		0.049 ± 0.0020	0.095 ± 0.008
		0.6*	—	3	-1.73	0.738	0.079 ± 0.0030	0.099 ± 0.005
				10	0		0.061 ± 0.0016	0.082 ± 0.006
				20	1		0.049 ± 0.0030	0.182 ± 0.003
		0.8	1	3	-1.73	0.360	0.063 ± 0.0073	0.134 ± 0.012
				10	0		0.046 ± 0.0023	0.072 ± 0.022
				20	1		0.020 ± 0.0027	0.097 ± 0.008
1500	1	0.2	-1	3	-1.73	2.480	0.051 ± 0.0027	0.021 ± 0.0004
				10	0		0.067 ± 0.0109	0.025 ± 0.002
				20	1		0.049 ± 0.0021	0.047 ± 0.006
		0.4	0	3	-1.73	1.958	0.053 ± 0.0021	0.037 ± 0.004
				10	0		0.052 ± 0.0035	0.055 ± 0.001
				20	1		0.045 ± 0.0026	0.072 ± 0.011
		0.6*	—	3	-1.73	1.472	0.050 ± 0.0138	0.067 ± 0.001
				10	0		0.041 ± 0.0074	0.057 ± 0.006
				20	1		0.030 ± 0.0080	0.092 ± 0.003
		0.8	1	3	-1.73	0.713	0.051 ± 0.0053	0.072 ± 0.001
				10	0		0.031 ± 0.0088	0.043 ± 0.006
				20	1		0.030 ± 0.0170	0.043 ± 0.007

Table 1. PE_{μ} of *Chlamydomonas* and *Chlorella* under the experimental matrix of light regimes. All data are the mean of 3 replicates \pm standard deviation. *Indicates data used for model validation. 'Coded' refers to the normalised values used for the quadratic model (Equation 2).

Light screen experiments were conducted over 3 days in a controlled semi-continuous cultivation regime. As light acclimation occurs on a timescale of several hours to days, sufficient time was given for the cells to acclimate to the light regime that they were exposed to. To minimise cell shading effects with increasing OD, cultures were diluted back to the same initial OD_{750} of 0.1 (pathlength 5 mm) each day. Quasi-steady-state growth rates, μ (h^{-1}) were calculated (Equation 3) from 3-hourly OD_{750} measurements (Supplementary Figs S1 and S2) on Day 2 during the exponential phase (after \sim 38 hours of light regime exposure) and normalised to the light received to estimate the photosynthetic efficiency (PE_{μ}) (Equation 4).

Photosynthetic efficiency under different light regimes. The PE_{μ} of *Chlamydomonas* and *Chlorella* under all 27 fluctuating light regimes are shown in Fig. 2A and B. Some similarities in the general trends of *Chlamydomonas* and *Chlorella* are evident, such as the effect of I_{\max} , where a large increase in PE_{μ} occurred with decreasing I_{\max} . To better depict PE_{μ} trends, individual treatments were averaged for each species over all factors (Fig. 2C), and over all but one factor (Fig. 2D–F). Overall, *Chlorella* exhibited a \sim 50% higher PE_{μ} than *Chlamydomonas* (average PE_{μ} of 0.099 ± 0.060 mol photon $^{-1}$ m 2 and 0.066 ± 0.034 mol photon $^{-1}$ m 2 respectively, Fig. 2C), in line with previous reports³².

Figure 2C also shows the mean PE_{μ} obtained under constant light was \sim 80% higher in *Chlamydomonas* but approximately the same for *Chlorella* (-7.5%) than that obtained under fluctuating light of the same I_{avg} . For *Chlamydomonas*, this result concurs with other studies showing a negative impact of fluctuating light on

	Coefficients from the quadratic non-linear model					
	PE _μ (10 ⁻³)		Φ _{PSII} (10 ⁻³)		F _v /F _m (10 ⁻³)	
	<i>Chlamydomonas</i>	<i>Chlorella</i>	<i>Chlamydomonas</i>	<i>Chlorella</i>	<i>Chlamydomonas</i>	<i>Chlorella</i>
D _f	-21.0*	20.5*	-35.7*	-8.1*	16.4*	16.6*
I _{max}	-20.0*	-61.2*	-3.2	-4.4	22.1*	-54.2*
t _c	-6.6	-5.5*	-3.3	-2.0	-0.9	-6.8*
D _f - I _{max}	16.0*	-10.3*	-29.6*	-6.8*	-6.1	9.7*
D _f - t _c	-1.1	-14.7*	0.8	0.9	-3.6	3.9
I _{max} - t _c	3.2	-9.5*	-5.0*	3.9	3.0	-6.5*
D _f ²	-24.6*	2.4	-26.8*	-4.7	10.4	1.8
I _{max} ²	14.2*	28.0*	19.1*	-4.9	31.8*	1.7
t _c ²	1.0	2.8	-0.2	0.6	1.7	-3.8
Intercept	67.6	71.1	236.5	194.3	655.6	647.1
R ²	0.67	0.93	0.89	0.44	0.74	0.91

Table 2. Comparison of the factor coefficients of the quadratic model obtained from analysis of variance (ANOVA) for A) PE_μ, B) Φ_{PSII} and C) F_v/F_m parameters for *Chlamydomonas* and *Chlorella*. *Represents significant effects at p-value < 0.05. n = 3 (PE_μ), n = 2 (Φ_{PSII} & F_v/F_m).

time-integrated photosynthesis and growth rates^{10,12,33,34}. Interestingly, for this strain of *Chlorella*, fluctuating light had little effect compared to constant light conditions.

For main effects of each factor, Fig. 2D shows at the lowest I_{max} value, the mean PE_μ increased up to two-fold for *Chlamydomonas* and 3.67-fold for *Chlorella*, respectively, indicating that photosynthetic light utilisation is compromised under high incident light (i.e. at noon under outdoor conditions)^{35–37}, especially for *Chlorella*.

The trends of D_f (Fig. 2E) resulted in diametrically opposing responses: PE_μ in *Chlamydomonas* performed best at a low D_f (increasing up to 83% from D_f = 0.8 to D_f = 0.2) while *Chlorella* at a high D_f (PE_μ increased up to 58% from D_f = 0.2 to D_f = 0.8). Since mass cultures operating under high cell densities is advantageous to reduce downstream processing costs, these results suggest that *Chlorella* is more suited to mass cultivation than *Chlamydomonas*.

For both species, the effect of t_c seemed minor (Fig. 2F). Cell cycling in the range analysed (t_c = 3, 10, 20 s) exhibited a modest increase in PE_μ with decreasing t_c values (39% for *Chlamydomonas* and 13% for *Chlorella*). While large improvements of PE_μ have been reported under sub-second cycle times approaching the ‘flashing light effect’^{28,38,39}, this is in line with other studies that have reported similar modest improvements for *Chlamydomonas* below cycle times of 10 s¹² and little effect in the seconds range for other *Chlorella* sp. and other algae^{11,38}.

Modelling light factor interactions using response surface methodology. Response surface methodology of the complete factorial design^{40–45} was next employed to model and explore the interactions between the three input factors (I_{max}, D_f and t_c) to PE_μ. Furthermore, to determine the influence of photoregulation under fluctuating light on PE_μ, supporting parameters at the level of PSII regulation for *Chlamydomonas* and *Chlorella* were also modelled from chlorophyll fluorescence data. These are: the operating efficiency of PSII (φ_{PSII}) – a measure of the proportion of absorbed light used for photochemistry; maximum quantum efficiency of PSII photochemistry (F_v/F_m) – an indicator of PSII inactivation via photoinhibition; and non-photochemical quenching (NPQ) – the apparent rate constant for heat loss from PSII⁴⁴. These parameters provide clues as to the underlying mechanisms of the observed PE_μ.

The three levels of each factor (Table 1) were coded with the mid-point (coded as ‘0’) and this was halved and doubled in the experimental design such that the coded factors of the independent variables were calculated using the logarithmic equation,

$$x_i = (1.4427 \ln(X_i) + A_i) \quad (1)$$

where, x is the coded factor level, X is the actual value of the factor, $i = 1, 2, 3$; A is the intercept value of the logarithmic function for each factor with $A_1 = 1.3219$, $A_2 = -9.5507$ and $A_3 = -3.3219$ for D_f, I_{max} and t_c respectively.

Quadratic models (Equation 2) were fitted to the data:

$$Y = \beta_0 + \sum_{i=1}^k \beta_i x_i + \sum_{i=1}^{k-1} \sum_{j=i+1}^k \beta_{ij} x_i x_j + \sum_{i=1}^k \beta_{ii} x_i^2 \quad (2)$$

In Equation 2, Y is the predicted response variable (PE_μ, φ_{PSII}, F_v/F_m or NPQ); β_0 , β_i , β_{ij} and β_{ii} are the coefficients for intercept, linear, interaction and quadratic effects respectively; $x_1, x_2 \dots x_k$ are the coded values of the input factors ($i \neq j$); and $k = 3$. Multiple regression of the data was used to obtain the regression coefficients.

*Model validation shows that the light factors I_{max}, D_f and t_c can be used to predict PE_μ accurately in *Chlorella* and moderately in *Chlamydomonas*.* For the primary response, PE_μ, the quadratic model demonstrated a moderate and high goodness of fit for *Chlamydomonas* (R² = 0.67) and *Chlorella* (R² = 0.93), respectively.

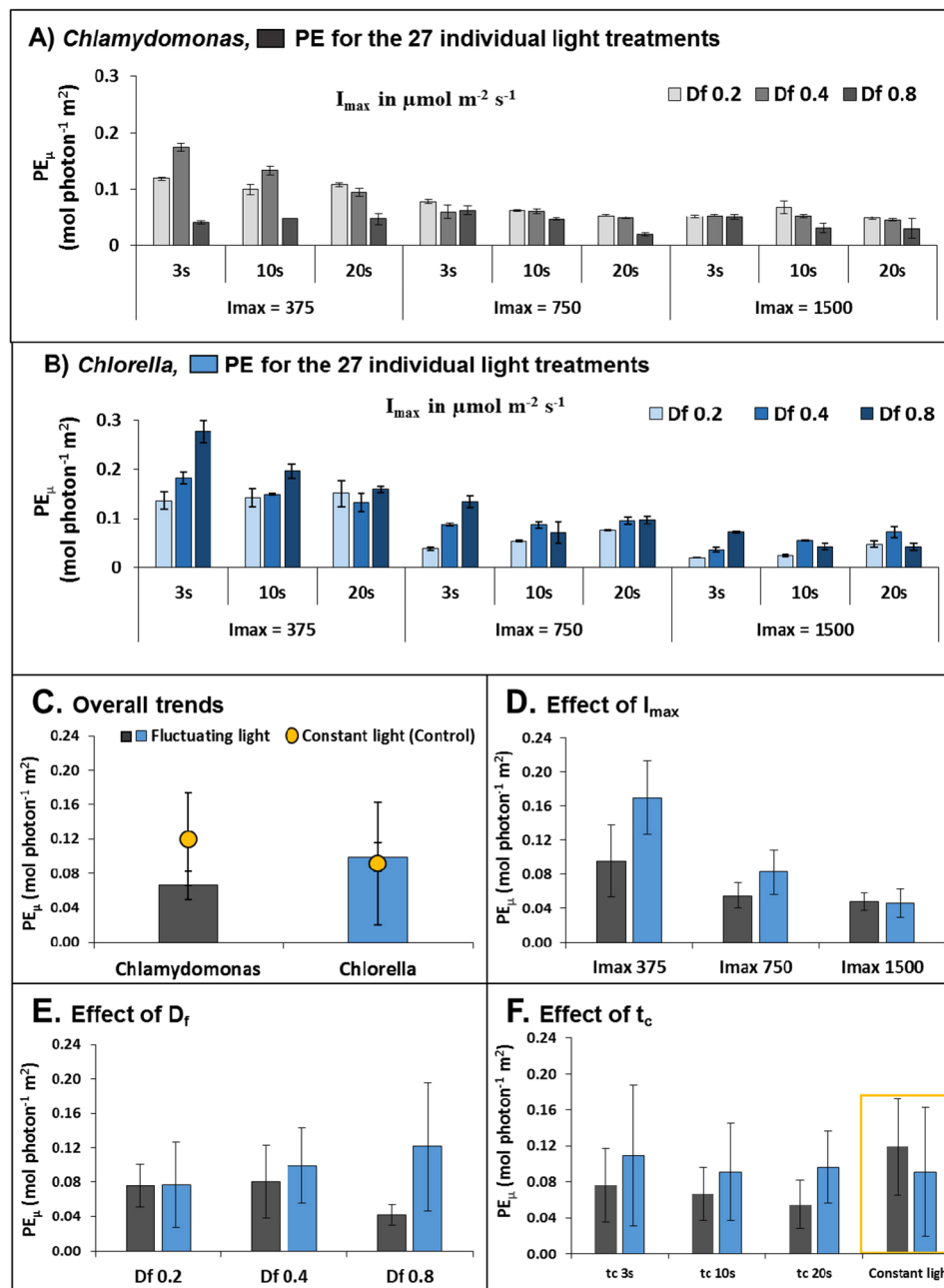


Figure 2. Trends in photosynthetic efficiency (PE_{μ}) under different light regimes of *Chlamydomonas* (grey bars) and *Chlorella* (blue bars). (A and B) individual PE_{μ} data of the 27 light treatments for *Chlamydomonas* and *Chlorella*, respectively ($n = 3$), (C) the overall trends in averaged PE_{μ} values over all conditions of D_f , I_{\max} and t_c tested ($n = 27$), (D) the averaged PE_{μ} values of D_f and t_c combined to show effect of I_{\max} ($n = 9$), (E) the averaged PE_{μ} values of I_{\max} and t_c combined to show effect of D_f ($n = 9$) and (F) the averaged PE_{μ} values of D_f and I_{\max} combined to show effect of t_c ($n = 9$). Error bars represent the standard deviation (SD) of individual treatments within biological triplicates (A,B) and between different treatments (C–F).

To assess whether the model fit was adequate to predict PE_{μ} within the range analysed, the quadratic models were validated using an additional set of experimental data at $D_f = 0.6$ at each level of I_{\max} and t_c (9 experimental sets for each strain) (Table 1). Comparing the fitted models against the actual data gave a low R^2 of 0.456 for *Chlamydomonas* and a high R^2 of 0.882 for *Chlorella* (Supplementary Fig. S5). In general, the residuals showed a normal distribution and the Cook's distance plot showed only a small number of outliers for *Chlamydomonas* and *Chlorella* (Supplementary Fig. S5).

For *Chlorella*, these results indicated that the three light factors accounted for a high proportion of variation in PE_{μ} observed and can be used to adequately predict their relationship to PE_{μ} . For *Chlamydomonas*, it seems there are more complex regulations of the photosynthetic machinery, which cannot be modelled with these factors alone.

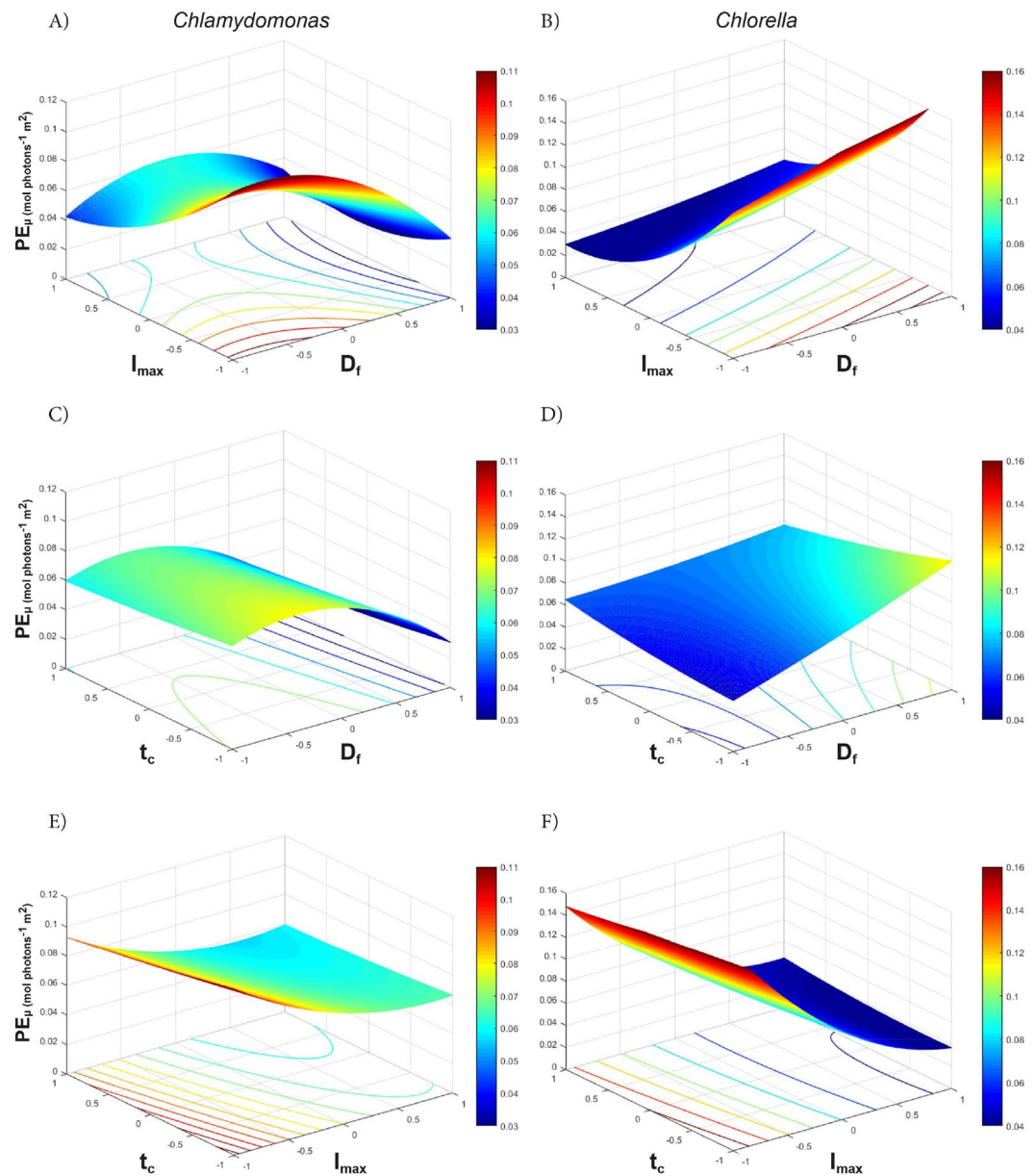


Figure 3. Response surface (3D) and contour (2D) plots of two-way interactions of factors affecting the PE_{μ} ($\text{mol photon}^{-1} \text{m}^{-2}$) of *Chlamydomonas* (A,C,E) and *Chlorella* (B,D,F). The colour bar depicts high PE_{μ} values in red and lower PE_{μ} values in blue.

The light factors of I_{\max} and D_f significantly affect PE_{μ} under fluctuating light. The coefficient terms tabulated in Table 2 show the relative size and direction that effect each factor has on the response variables, while the three dimensional (3D) response surface plots and 2D contour plots graphically depict the interactions of two factors on the primary response of PE_{μ} , where the third factor is set to the midpoint (Fig. 3).

For *Chlamydomonas*, the most significant factors affecting PE_{μ} were: I_{\max} (p-value = $3.83E^{-08}$), D_f (p-value = $1.04E^{-08}$), and the interaction of D_f - I_{\max} (p-value $1.05E^{-04}$) (Table 2). Here, both high D_f and high I_{\max} had similar negative impacts on PE_{μ} , yet the interaction of D_f - I_{\max} had a positive effect, suggesting that dense cultures may offer some protection under high light whilst dilute cultures may improve PE_{μ} under low light. As expected, the 3D plots show the highest PE_{μ} values at a combination of low D_f (i.e. not light limited) and low I_{\max} (i.e. not photo-inhibited) (Fig. 3A), however, the slight saddle shape of the interaction plot at high I_{\max} shows that the optimal D_f is around 0.4 (at the mid-point) for *Chlamydomonas*.

The PE_{μ} of *Chlorella* was most significantly adversely affected by high I_{\max} (p-value $9.92E^{-37}$), and unlike *Chlamydomonas*, showed a significant positive response for increasing D_f (p-value $4.67E^{-12}$). The I_{\max} - D_f interaction showed an exponential increase in PE_{μ} with a reduction of I_{\max} and an increase in D_f (Fig. 3B). However, the significant negative interaction of D_f - t_c (Table 2) suggests that long cycle times could adversely affect productivity

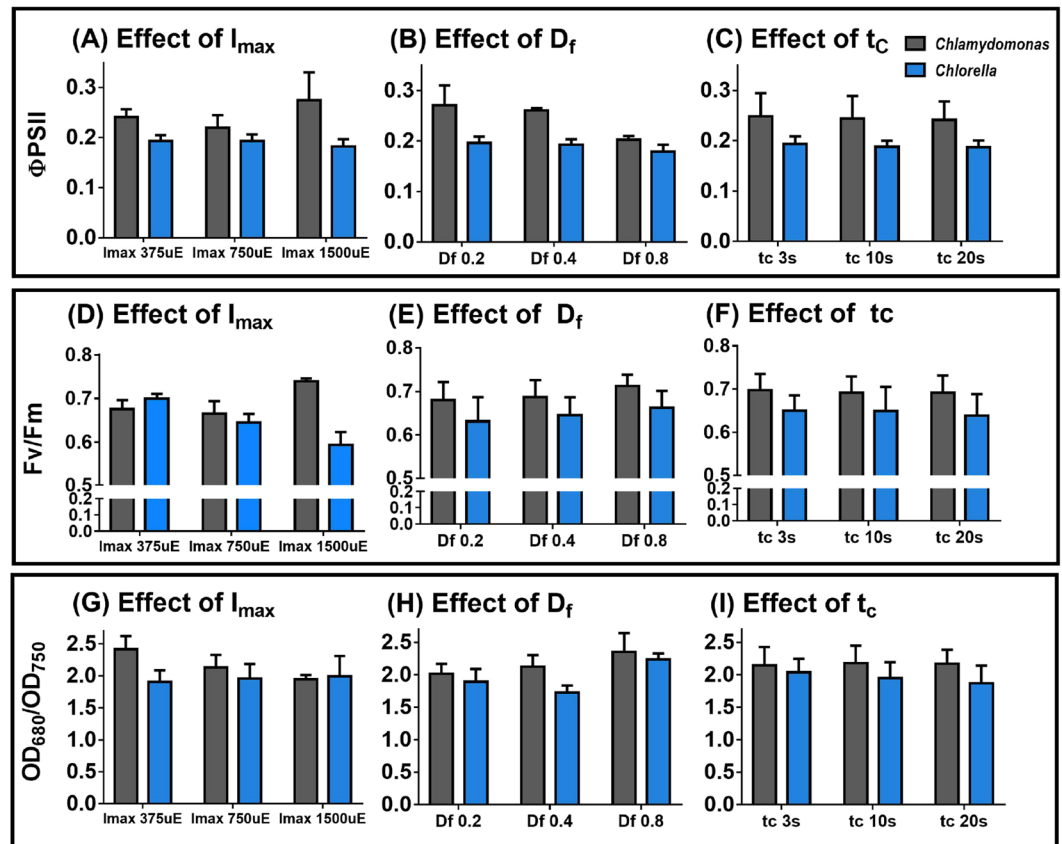


Figure 4. Trends in underlying photosynthetic mechanisms. Plots depict averaged effects of I_{\max} , D_f and t_c on Φ_{PSII} (A,B and C) ($n = 2$); F_v/F_m (D,E and F) and $\text{OD}_{680}/\text{OD}_{750}$ (G,H and I) respectively for *Chlamydomonas* (grey bars) and *Chlorella* (blue bars) ($n = 3$, Error bars represent standard deviation).

in high density cultures (Fig. 3D). Overall, for *Chlamydomonas* a low I_{\max} and low D_f (Fig. 3A) and for *Chlorella* a low I_{\max} and high D_f (with moderate benefits of low t_c) (Fig. 3 B and D) resulted in the highest PE_{μ} .

PSII regulation has a strong effect on PE_{μ} under fluctuating light. To assess some underlying mechanisms that may affect PE_{μ} , chlorophyll fluorescence measurements were taken to assess levels of stress and photo-inhibition (F_v/F_m), the operating efficiency of PSII (Φ_{PSII}) and non-photochemical quenching (NPQ). The data was fitted to the quadratic model (Equation 2) to compare the magnitude of effect of the three light factors. Additionally, changes in the ratio of $\text{OD}_{680}/\text{OD}_{750}$ were used as a high-throughput proxy to determine photoacclimation via changes in chlorophyll content.

A high goodness of fit to the quadratic model was observed in *Chlamydomonas* for Φ_{PSII} ($R^2 = 0.89$) and F_v/F_m ($R^2 = 0.74$) and, in *Chlorella*, for F_v/F_m ($R^2 = 0.91$), suggesting that PSII regulation is highly affected by the three light factors examined in this study and is a contributing factor to the observed PE_{μ} . Remarkably, all treatments for both species showed low NPQ (< 0.3) relative to average values reported in literature (up to ~ 2 for *Chlamydomonas* and ~ 1.5 for *Chlorella*)^{15,46–48} and a poor goodness of fit to the quadratic model for both strains (see Supplementary Table S2). Other stressors, such as nutrient limitation, are also known to increase NPQ⁴⁹. Since both strains were cultivated on previously optimised nutrients this may have contributed to the overall reduced NPQ in this study.

For *Chlamydomonas*, a significant (p -value = $1.79\text{E-}17$) reduction in Φ_{PSII} occurred at high D_f (Table 2, Fig. 2E). This suggests that efficient electron transfer is compromised under high dark fractions for this alga and links Φ_{PSII} to the reduced PE_{μ} trends under high D_f observed. Furthermore, increased $\text{OD}_{680}/\text{OD}_{750}$ measurement (a proxy for chlorophyll content per cell) was prominent with increasing D_f (Fig. 4H), suggesting high dark fractions lead to increased cellular chlorophyll levels typical for low-light acclimation, which may further explain the lower efficiency of light utilisation (i.e. PE) at high D_f (Fig. 2E). Remarkably, a high I_{\max} actually improved both Φ_{PSII} (Fig. 4A) and F_v/F_m (Fig. 4D) and lowered $\text{OD}_{680}/\text{OD}_{750}$ (Fig. 4G), despite a reduction in PE_{μ} (Fig. 2D). This suggests that while photosynthetic rates improved in *Chlamydomonas* under high light, the over-saturating irradiance could not be fully utilised by the Calvin-Benson cycle, suggesting other downstream mechanisms such as alternative electron sinks⁵⁰ could become relevant under high light.

For *Chlorella*, the most significant factor corresponding directly to PE_{μ} was the effect of I_{\max} on F_v/F_m , which gave a large negative coefficient in the model (Table 2) and showed a noticeable decline in F_v/F_m with increasing I_{\max} (Fig. 4D). Like *Chlamydomonas*, increasing D_f was found to have a positive effect on F_v/F_m (Fig. 4E),

Species	Condition	Predicted max PE _μ	D _f		I _{max}		t _c	
		(mol photon ⁻¹ m ⁻²)	Coded	(-)	Coded	(μmol m ⁻² s ⁻¹)	Coded	(s)
<i>Chlamydomonas</i>	t _c midpoint	0.116	-0.75	0.24	-1	375	0	10
	I _{max} midpoint	0.079	-0.4	0.30	0	750	-1	5
	D _f midpoint	0.113	0	0.40	-1	375	-1	5
	Optima	0.126	-0.73	0.24	-1	375	-1	5
<i>Chlorella</i>	t _c midpoint	0.194	1	0.80	-1	375	0	10
	I _{max} midpoint	0.117	1	0.80	0	750	-1	5
	D _f midpoint	0.178	0	0.40	-1	375	-1	5
	Optima	0.226	1	0.80	-1	375	-1	5

Table 3. Optimisation of PE_μ and the respective factor levels around the mid-point of each factor, and around the optimised point for total predicted maximum PE_μ within the ranges of the full factorial design.

also seen by the relative magnitudes of coefficients and their significance (p -value = 3.09E-07), and a significant positive interaction between D_f – I_{max} (p -value = 5.19E-03). Similar to *Chlamydomonas*, *Chlorella* exhibited an up-regulation of OD_{680/750} (indicative of higher chlorophyll) at high D_f (Fig. 4H, Supplementary Table S2).

In summary, these results suggest that *Chlorella* is sensitive to high light as seen by PSII inactivation but less sensitive to light/dark fluctuations. In contrast, *Chlamydomonas* is sensitive to strong light/dark fluctuations due to disrupted electron transport flows but seems to have better acclimatisation strategies to cope with high light. These results suggest that maintaining *Chlamydomonas* at relatively dilute cultures is beneficial, whereas operating *Chlorella* at high densities is preferable, especially under high light.

Optimisation predicts a two-fold higher maximum PE_μ for *Chlorella* compared to *Chlamydomonas*.

It is evident from the 3D surface plots (Fig. 3) showing PE_μ response that the maxima occur at the extremes in most instances. The maximum PE_μ values (at the mid-point, i.e. level 0) and their corresponding factor levels were used to obtain the maximum PE_μ and optimum conditions. For both *Chlamydomonas* and *Chlorella*, the maximum PE_μ values occurred at the minimum I_{max} (375 μE) and the minimum value of t_c (Table 3). Using this combination of I_{max} and t_c, the optimal D_f values were found to be 0.24 and 0.8 for *Chlamydomonas* and *Chlorella* respectively. These combination of factor values results in a theoretical maximum PE_μ of 0.126 and 0.226 mol photon⁻¹ m⁻² (Table 3), predicting a nearly 2-fold higher maximum PE_μ for *Chlorella* than *Chlamydomonas*. As discussed in the section 3.3.1, the three light factors modelled only explains two thirds of the variation in PE_μ for *Chlamydomonas* and these results are indicative only for this species.

Concluding Remarks

The HTS coupled with response surface methodology delivers a working statistical design for simultaneous light optimisation of several species of microalgae. This platform has been used to screen growth responses to nutrients and organic carbon sources^{20,23}, and can be extended to screen other parameters such as CO₂ or growth contaminants (e.g. herbicides, antibiotics, bacteria or predating organisms), and could monitor other response variables such as lipid accumulation (e.g. Nile Red) and protein expression using fluorescence tags. Some limitations imposed by the microwell HTS can include high variation between replicates when trialled at conditions that give very low growth rates; and some evaporation losses that limit the duration of the experiment due to the low culture volume. Radzun, K. A. *et al.* have reported that despite some evaporative losses observed in the TECAN robotic system, the RSD values were considerably lower than can be achieved through manual measurement.

As the OD measurements in the plate reader are made vertically rather than horizontally, the reduction of depth due to evaporation is compensated for by the concomitant increase in cell concentration to maintain the same optical pathlength²³. Furthermore, variation can be reduced by adding additional technical replicates (as done in this study), while evaporation can be addressed by using a humidifier in the enclosed chamber system (currently being developed) and/or reducing the frequency of measurement readings which requires lid removal. Despite this, the HTS provides a cost-effective, rapid and efficient platform to obtain large data-sets for a wide array of solar driven microalgae applications, which would otherwise require significant investment of time, money and resources.

In most mass cultures, particularly those of outdoor raceway ponds, severe light limitation exists, typically where light penetrates only the first millimetres or centimetres at most and high dark fractions of 90% or greater are normal^{24,30}. These dark fractions and cycling between light/dark zones can be detrimental for redox imbalances, as was shown to be the case for *Chlamydomonas*. Therefore, species such as the strain of *Chlorella* tested here, have a selective advantage for mass culture, as productivity was found to be unaffected by light fluctuations. Furthermore, it opens up new insights for the design of high efficiency cell lines, capable of handling both high light intensities and strong light/dark fluctuations. Improving light distribution deeper within the culture depth with minimal transmittance losses (e.g. by increasing surface to volume ratios or using specially designed light guides⁵¹) may be another strategy to improve PE_μ, rather than adjusting cycle time (by increasing mixing rates, gas sparging) particularly as the latter would require higher energy inputs with minimal gains in PE_μ. Another important deduction of strain-specific characterisation for scale up was the detrimental effect of cycle time on PE_μ for *Chlamydomonas* (~-46%) versus a similar effect for *Chlorella* as compared to constant light. This signifies the application of our HTS outcomes toward strain selection as well as growth platform selection (i.e. open pond (slow mixing) versus tubular PBRs (faster mixing) or other designs) when going from laboratory (constant light)

to outdoor systems (fluctuating light). In both alga, as is typical of other species, high incident light has the most detrimental effect on PE_{μ} . Therefore, efforts to diffuse light sources, such as done through the use of reflectors, or to use vertical flat panels or vertically stacked tubular photobioreactors to avoid direct sunlight at high light periods, may benefit from the 'light dilution effect'.

Previous transcriptomic and proteomic studies in *Chlamydomonas* have shown that acclimation to environmental stimuli is achieved by remodelling photosystem I and II antenna complexes, further highlighting the flexibility of their photosynthetic machinery⁵². While *Chlamydomonas* may possess the survival strategies required to acclimate to changing light conditions, typically for soil environments, they may not be tuned for high biomass productivity, unlike fast-growing strains like the *Chlorella* strain used in this study, which despite seemingly lacking the level of regulatory sophistication, might be better suited for mass cultivation.

In conclusion, the HTS method developed here enables a rapid approach to optimise systems design, scale up operational conditions and species selection to advance feasible solar-driven biotechnologies.

Materials and Methods

Strains and pre-culture conditions. Liquid pre-cultures were prepared in triplicate (40 mL culture in 100 mL flasks) and inoculated with either *C. reinhardtii* WT strain CC125⁵³ or *Chlorella* sp. 11_H5¹⁹ (Australian isolate) maintained on TAP⁵⁴ agar (1.5%) plates. To ensure nutrients were non-limiting, photoautotrophic medium previously optimised for each species was used for *C. reinhardtii* (PCM⁵⁵, N source NH_4^+) and *Chlorella* sp (OpM₂²⁰, N source urea). Flasks were maintained on shakers (200 rpm) in an enclosed incubation system at 23 °C, 1% CO_2 and a 16/8 hour light/dark cycle, illuminated with 100 $\mu mol m^{-2} s^{-1}$ of overhead white fluorescent light for 5 days.

To ensure that the cultures were well synchronised to the light conditions being tested, flask pre-cultures first acclimated to a 16/8 h light/dark cycle were inoculated into microwell plates (150 μL), and gradually acclimated to the light intensity close to the mean I_{avg} before the first measurement. For the higher light intensity experiments ($I_{max} = 1500 \mu mol m^{-2} s^{-1}$), care was taken not to shock the low density cultures by subjecting them to a step-wise gradually increasing light regime (a detailed summary of the acclimation regimes is provided in Supplementary Table S3).

Automated HTS and lighting design. The design, structure and operation of the HTS system (Tecan Freedom Evo 150, Tecan Group Ltd., Männedorf, Switzerland) is as previously described^{20,23}. Briefly, the HTS system is an enclosed chamber fitted with three orbital shakers which hold six microwell plates each, a robotic manipulator arm that removes the plate lid and carries the plates to a reader (Infinite M200 PRO, Tecan Group Ltd., Männedorf, Switzerland, Fig. 1C) and atmospheric CO_2 control. Each of the 18 microwell plate positions is fitted with 96 'warm white' LEDs positioned directly under each well of a 96-well plate. Each of the LED arrays is controlled by user defined scripts on an Arduino[®] integrated circuit controller and software, permitting 18 different light conditions to be tested in parallel. LEDs were fitted with a low pass LC filter to smooth the intensity signal from pulse width modulation to variable voltage, thereby eliminating 'flashing light' phenomena due to on/off signals. The spectrum of wavelengths of LEDs is compared against that of natural sunlight (see Supplementary Fig. S6). For simplicity, a sinusoidal mixing regime was assumed to allow tight control of the factors of I_{max} , D_f and t_c , as has been used in previous studies^{36,37}. Pre-cultures were centrifuged (500 g, 20 min, 18 °C) and the pellet re-suspended in fresh medium. To minimise cell shading effects and ensure tight light control, a volume of 150 μL was chosen for a short pathlength of 5 mm and a semi-continuous cultivation regime was applied by daily culture dilutions back to a starting OD_{750} of 0.1. Each of the three biological replicates per species was inoculated into each well of a 96-well plate. Since only two strains were tested in this study, all wells were inoculated, providing 14 technical replicates per biological replicate. Of these, 10 wells were used for automated OD_{750} and OD_{680} readings, the remaining wells (of two biological replicates) were extracted on day 2 for manual PSII measurements. The final row of 12 wells contained 150 μL pure media to use as blank controls.

Growth rate and photosynthetic efficiency (PE_{μ}) measurements. Growth rates were calculated from 3-hourly OD_{750} measurements. High-throughput automated measurements of OD_{750} were used as a proxy for growth from which growth rates, μ (h^{-1}), were calculated as the rate of change of OD_{750} ,

$$\mu = (\ln OD_{750}(t_2) - \ln OD_{750}(t_1)) / (t_2 - t_1) \quad (3)$$

where, t_1 and t_2 are the time points at which $OD_{750}(t_1)$ and $OD_{750}(t_2)$ were measured.

A 3-hour measuring frequency during the light period was used for the growth curve calculations. This frequency was chosen to limit evaporation and contamination issues. A detailed description of the growth curves, sampling points and lighting schedule can be found as Supplementary Figs S1 and S2.

The main response variable, PE_{μ} , was assumed to be indicative of light utilisation efficiency of the microalgae, where the growth rate normalised to the average integrated PAR received,

$$PE = \mu / I_{avg} \quad (4)$$

And the I_{avg} is,

$$I_{avg} = \int_0^t I(t) dt * 3.6 * 10^{-9} \quad (5)$$

In Equation 5, t_c is the cycle time, $I(t)$ is the irradiance ($\mu mol photons m^{-2} s^{-1}$) at a given time of t_c , and $3.6 * 10^{-9}$ is the conversion factor from $\mu mol photons m^{-2} s^{-1}$ to $mol photons m^{-2} h^{-1}$.

Chlorophyll fluorescence of photosystem II measurements. Photosystem II (PSII) kinetics were measured as a function of PSII chlorophyll fluorescence^{10,58,59}. Biological duplicates of each sample (dilution factor of 5) was added to a Fluorimeter cuvette (Sigma), dark adapted for 20 minutes and processed using the FluoroWin software (Photon Systems Instruments, Czech Republic). The quenching analysis protocol had the following settings: measuring light: 20% V; saturating pulse: 0.9 s, 80% V; actinic light: 51 s, 18.3 V (~800 $\mu\text{mol m}^{-2} \text{s}^{-1}$). Weak infrared pulses (730 nm) were applied for 5 s prior to measurement to quench Q_A . The PSII parameters calculated from the quenching analysis were: F_v/F_m (maximum quantum efficiency of PSII), Φ_{PSII} (PSII operating efficiency), and NPQ (Non photochemical Quenching) using respectively,

$$F_v/F_m = (F_m - F_0)/F_m \quad (6)$$

$$\Phi_{PSII} = (F'_m - F)/F'_m \quad (7)$$

$$NPQ = (F_m/F'_m) - 1 \quad (8)$$

Photoacclimation via OD_{680/750}. Chlorophyll *a* has a maximum absorbance at 680 nm. Therefore, OD₆₈₀ measurements were normalised to OD₇₅₀ (OD_{680/750}) as a proxy of changes in chlorophyll absorption between different light regimes.

Statistical Analysis. All data are expressed as Mean \pm SD of three biological replicates (for automated readings) and two biological replicates (for the manual PSII measurements), each with multiple technical replicates as mentioned in section 5.2. MATLAB was used for the design and analysis of the response surface methodology. A p-value <0.05 was used for determining significant effects. Both contour and surface plots were developed for visualisation of the data and to predict the relationship and interaction effects on the light utilisation efficiency. Regression coefficient (R^2) was used to resolve the goodness of fit. The fitted model using the regression coefficients was validated with an additional experimental dataset.

References

- Singh, S., Kate, B. N. & Banerjee, U. C. Bioactive Compounds from Cyanobacteria and Microalgae: An Overview. *Critical Reviews in Biotechnology* **25**, 73–95, <https://doi.org/10.1080/07388550500248498> (2005).
- Borowitzka, M. *High-value products from microalgae—Their development and commercialisation*. Vol. 25 (2013).
- Carrera Pacheco, S. E., Hankamer, B. & Oey, M. Optimising light conditions increases recombinant protein production in *Chlamydomonas reinhardtii* chloroplasts. *Algal Research* **32**, 329–340, <https://doi.org/10.1016/j.algal.2018.04.011> (2018).
- Koutra, E., Economou, C. N., Tsafrakidou, P. & Kornaros, M. Bio-Based Products from Microalgae Cultivated in Digestates. *Trends in Biotechnology*. <https://doi.org/10.1016/j.tibtech.2018.02.015> (2018).
- Chew, K. W. *et al.* Microalgae biorefinery: High value products perspectives. *Bioresource Technology* **229**, 53–62, <https://doi.org/10.1016/j.biortech.2017.01.006> (2017).
- Béchet, Q., Plouviez, M., Chambonnière, P. & Guieysse, B. In *Microalgae-Based Biofuels and Bioproducts* (ed. Raúl Muñoz) 505–525 (Woodhead Publishing, 2017).
- Stephens, E. *et al.* An economic and technical evaluation of microalgal biofuels. *Nat Biotech* **28**, 126–128, <https://doi.org/10.1038/nbt0210-126> (2010).
- Ringsmuth, A. K., Landsberg, M. J. & Hankamer, B. Can photosynthesis enable a global transition from fossil fuels to solar fuels, to mitigate climate change and fuel-supply limitations? *Renewable and Sustainable Energy Reviews* **62**, 134–163, <https://doi.org/10.1016/j.rser.2016.04.016> (2016).
- Mussgnug, J. H. *et al.* Engineering photosynthetic light capture: impacts on improved solar energy to biomass conversion. *Plant Biotechnology Journal* **5**, 802–814, <https://doi.org/10.1111/j.1467-7652.2007.00285.x> (2007).
- Yarnold, J., Ross, I. L. & Hankamer, B. Photoacclimation and productivity of *Chlamydomonas reinhardtii* grown in fluctuating light regimes which simulate outdoor algal culture conditions. *Algal Research* **13**, 182–194, <https://doi.org/10.1016/j.algal.2015.11.001> (2016).
- Barbosa, M. J., Hoogakker, J. & Wijffels, R. H. Optimisation of cultivation parameters in photobioreactors for microalgae cultivation using the A-stat technique. *Biomolecular Engineering* **20**, 115–123, [https://doi.org/10.1016/S1389-0344\(03\)00033-9](https://doi.org/10.1016/S1389-0344(03)00033-9) (2003).
- Takache, H., Pruvost, J. & Marec, H. Investigation of light/dark cycles effects on the photosynthetic growth of *Chlamydomonas reinhardtii* in conditions representative of photobioreactor cultivation. *Algal Research* **8**, 192–204, <https://doi.org/10.1016/j.algal.2015.02.009> (2015).
- Senge, M. & Senger, H. Response of the Photosynthetic Apparatus during Adaptation of *Chlorella* and *Ankistrodesmus* to Irradiance Changes. *Journal of plant physiology* **136**, 675–679, [https://doi.org/10.1016/S0176-1617\(11\)81343-X](https://doi.org/10.1016/S0176-1617(11)81343-X) (1990).
- Hosni, T., Gwendoline, C., Jean-François, C. & Jérémy, P. Experimental and theoretical assessment of maximum productivities for the microalgae *Chlamydomonas reinhardtii* in two different geometries of photobioreactors. *Biotechnology progress* **26**, 431–440, <https://doi.org/10.1002/btpr.356> (2010).
- Peers, G. *et al.* An ancient light-harvesting protein is critical for the regulation of algal photosynthesis. *Nature* **462**, 518–521 (2009).
- Merchant, S. S. *et al.* The *Chlamydomonas* Genome Reveals the Evolution of Key Animal and Plant Functions. *Science* **318**, 245–250, <https://doi.org/10.1126/science.1143609> (2007).
- Mayfield, S. P. *et al.* *Chlamydomonas reinhardtii* chloroplasts as protein factories. *Current Opinion in Biotechnology* **18**, 126–133, <https://doi.org/10.1016/j.copbio.2007.02.001> (2007).
- Oey, M., Ross, I. L. & Hankamer, B. Gateway-Assisted Vector Construction to Facilitate Expression of Foreign Proteins in the Chloroplast of Single Celled Algae. *PLOS ONE* **9**, e86841, <https://doi.org/10.1371/journal.pone.0086841> (2014).
- Wolf, J. *et al.* Multifactorial comparison of photobioreactor geometries in parallel microalgae cultivations. *Algal Research* **15**, 187–201, <https://doi.org/10.1016/j.algal.2016.02.018> (2016).
- Wolf, J. *et al.* High-throughput screen for high performance microalgae strain selection and integrated media design. *Algal Research* **11**, 313–325, <https://doi.org/10.1016/j.algal.2015.07.005> (2015).
- Harris, E. H. *The Chlamydomonas Sourcebook: Introduction to Chlamydomonas and Its Laboratory Use*. (Elsevier Science, 2009).
- Moejes, F. W. *et al.* A systems-wide understanding of photosynthetic acclimation in algae and higher plants. *Journal of Experimental Botany* **68**, 2667–2681, <https://doi.org/10.1093/jxb/erx137> (2017).

23. Radzun, K. A. *et al.* Automated nutrient screening system enables high-throughput optimisation of microalgae production conditions. *Biotechnology for Biofuels* **8**, 65, <https://doi.org/10.1186/s13068-015-0238-7> (2015).
24. Richmond, A. In *Handbook of Microalgal Culture* 169–204 (John Wiley & Sons, Ltd, 2013).
25. Larkum, A. W. D. Limitations and prospects of natural photosynthesis for bioenergy production. *Current Opinion in Biotechnology* **21**, 271–276, <https://doi.org/10.1016/j.copbio.2010.03.004> (2010).
26. Masojídek, J., Sergejevoá, M., Malapascua, J. R. & Kopecký, J. In *Algal Biorefineries: Volume 2: Products and Refinery Design* (eds Aleš Prokop, Rakesh K. Bajpai, & Mark E. Zappi) 237–261 (Springer International Publishing, 2015).
27. Janssen, M. *et al.* Scale-up aspects of photobioreactors: effects of mixing-induced light/dark cycles. *Journal of Applied Phycology* **12**, 225–237, <https://doi.org/10.1023/a:1008151526680> (2000).
28. Janssen, M., Slenders, P., Tramper, J., Mur, L. R. & Wijffels, R. Photosynthetic efficiency of *Dunaliella tertiolecta* under short light/dark cycles. *Enzyme Microb Tech* **29**, 298–305, [https://doi.org/10.1016/s0141-0229\(01\)00387-8](https://doi.org/10.1016/s0141-0229(01)00387-8) (2001).
29. Janssen, M. *et al.* Efficiency of light utilization of *Chlamydomonas reinhardtii* under medium-duration light/dark cycles. *Journal of Biotechnology* **78**, 123–137 (2000).
30. Yarnold, J. *Photosynthesis of microalgae in outdoor mass cultures and modelling its effects on biomass productivity for fuels, feeds and chemicals* PhD thesis, The University of Queensland (2016).
31. Bureau of Meteorology, www.bom.gov.au (2016).
32. Janssen, M. *et al.* Specific growth rate of *Chlamydomonas reinhardtii* and *Chlorella sorokiniana* under medium duration light/dark cycles: 13–87 s. *Journal of biotechnology* **70**, 323–333, [https://doi.org/10.1016/S0168-1656\(99\)00084-X](https://doi.org/10.1016/S0168-1656(99)00084-X) (1999).
33. K  hlheim, C.,   gren, J. & Jansson, S. Rapid regulation of light harvesting and plant fitness in the field. *Science* **297**, 91–93 (2002).
34. Kaiser, E., Morales, A. & Harbinson, J. Fluctuating Light Takes Crop Photosynthesis on a Rollercoaster Ride. *Plant Physiology* **176**, 977–989, <https://doi.org/10.1104/pp.17.01250> (2018).
35. Bonente, G., Pippa, S., Castellano, S., Bassi, R. & Ballottari, M. Acclimation of *Chlamydomonas reinhardtii* to different growth irradiances. *Journal of Biological Chemistry* **287**, 5833–5847, <https://doi.org/10.1074/jbc.M111.304279> (2012).
36. MacIntyre, H. L., Kana, T. M., Anning, T. & Geider, R. J. Photoacclimation of photosynthesis irradiance response curves and photosynthetic pigments in microalgae and cyanobacteria1. *J Physcol* **38**, 17–38, <https://doi.org/10.1046/j.1529-8817.2002.00094.x> (2002).
37. de Winter, L., Cabanelas, I. T. D., Martens, D. E., Wijffels, R. H. & Barbosa, M. J. The influence of day/night cycles on biomass yield and composition of *Neochloris oleoabundans*. *Biotechnology for Biofuels* **10**, 104, <https://doi.org/10.1186/s13068-017-0762-8> (2017).
38. Vejrazka, C., Janssen, M., Benvenuti, G., Streefland, M. & Wijffels, R. H. Photosynthetic efficiency and oxygen evolution of *Chlamydomonas reinhardtii* under continuous and flashing light. *Applied Microbiology and Biotechnology* **97**, 1523–1532, <https://doi.org/10.1007/s00253-012-4390-8> (2013).
39. Sforza, E., Simionato, D., Giacometti, G. M. & Bertuccio, A. & Morosinotto, T. Adjusted Light and Dark Cycles Can Optimize Photosynthetic Efficiency in Algae Growing in Photobioreactors. *Plos One* **7**, e38975, <https://doi.org/10.1371/journal.pone.0038975> (2012).
40. Box, G. E. P. & Behnken, D. W. Some New Three Level Designs for the Study of Quantitative Variables. *Technometrics* **2**, 455–475, <https://doi.org/10.1080/00401706.1960.10489912> (1960).
41. Belhaj, D. *et al.* Box-Behnken design for extraction optimization of crude polysaccharides from Tunisian *Phormidium versicolor* cyanobacteria (NCC 466): Partial characterization, *in vitro* antioxidant and antimicrobial activities. *International Journal of Biological Macromolecules* **105**, 1501–1510, <https://doi.org/10.1016/j.ijbiomac.2017.06.046> (2017).
42. Kennedy, M. & Krouse, D. Strategies for improving fermentation medium performance: a review. *Journal of Industrial Microbiology and Biotechnology* **23**, 456–475, <https://doi.org/10.1038/sj.jim.2900755> (1999).
43. Wang, B. & Lan, C. Q. Optimising the lipid production of the green alga *Neochloris oleoabundans* using box–behnken experimental design. *The Canadian Journal of Chemical Engineering* **89**, 932–939, <https://doi.org/10.1002/cjce.20513> (2011).
44. Zhao, L.-C. *et al.* Response Surface Modeling and Optimization of Accelerated Solvent Extraction of Four Lignans from *Fructus Schisandrae*. *Molecules* **17**, 3618 (2012).
45. Kasiri, S., Abdulsalam, S., Ulrich, A. & Prasad, V. Optimization of CO₂ fixation by *Chlorella kessleri* using response surface methodology. *Chemical Engineering Science* **127**, 31–39, <https://doi.org/10.1016/j.ces.2015.01.008> (2015).
46. Garcia-Mendoza, E., Matthijs, H. C. P., Schubert, H. & Mur, L. R. Non-photochemical quenching of chlorophyll fluorescence in *Chlorella fusca* acclimated to constant and dynamic light conditions. *Photosynthesis Research* **74**, 303, <https://doi.org/10.1023/a:1021230601077> (2002).
47. Finazzi, G. & Minagawa, J. In *Non-Photochemical Quenching and Energy Dissipation in Plants, Algae and Cyanobacteria* 445–469 (Springer, 2014).
48. Masojídek, J. *et al.* Photoadaptation of two members of the Chlorophyta (*Scenedesmus* and *Chlorella*) in laboratory and outdoor cultures: changes in chlorophyll fluorescence quenching and the xanthophyll cycle. *Planta* **209**, 126–135, <https://doi.org/10.1007/s004250050614> (1999).
49. Petroustos, D. *et al.* The Chloroplast Calcium Sensor CAS Is Required for Photoacclimation in *Chlamydomonas reinhardtii*. *The Plant Cell* **23**, 2950–2963, <https://doi.org/10.1105/tpc.111.087973> (2011).
50. Dep  ge, N., Bellafiore, S. & Rochaix, J.-D. Role of Chloroplast Protein Kinase Stt7 in LHClI Phosphorylation and State Transition in *Chlamydomonas*. *Science* **299**, 1572–1575, <https://doi.org/10.1126/science.1081397> (2003).
51. Kommareddy, A. & Gary Anderson, D. *Study of Light as a parameter in the growth of algae in a Photo-Bio Reactor (PBR)* (ASAE, St. Joseph, MI, 2003).
52. Eberhard, S., Finazzi, G. & Wollman, F.-A. The Dynamics of Photosynthesis. *Annual Review of Genetics* **42**, 463–515, <https://doi.org/10.1146/annurev.genet.42.110807.091452> (2008).
53. *Chlamydomonas Resource Centre*, <https://www.chlamycollection.org> (2016).
54. Gorman, D. S. & Levine, R. Cytochrome f and plastocyanin: their sequence in the photosynthetic electron transport chain of *Chlamydomonas reinhardtii*. *Proceedings of the National Academy of Sciences* **54**, 1665–1669 (1965).
55. Oey, M. *et al.* RNAi knock-down of LHCBM1, 2 and 3 increases photosynthetic H₂ production efficiency of the green alga *Chlamydomonas reinhardtii*. *PLoS One* **8**, e61375 (2013).
56. Fl  meling, I. A. & Kromkamp, J. Photoacclimation of *Scenedesmus protuberans* (Chlorophyceae) to fluctuating irradiances simulating vertical mixing. *Journal of Plankton Research* **19**, 1011–1024, <https://doi.org/10.1093/plankt/19.8.1011> (1997).
57. Ibelings, B. W. & Mur, L. R. Acclimation of Photosystem II in a Cyanobacterium and a Eukaryotic Green Alga to High and Fluctuating Photosynthetic Photon Flux Densities, Simulating Light Regimes Induced by Mixing in Lakes. *New Phytologist* **128**, 407–424, <https://doi.org/10.1111/j.1469-8137.1994.tb02987.x> (1994).
58. Murchie, E. H. & Lawson, T. Chlorophyll fluorescence analysis: a guide to good practice and understanding some new applications. *Journal of Experimental Botany* **64**, 3983–3998, <https://doi.org/10.1093/jxb/ert208> (2013).
59. Baker, N. R. Chlorophyll Fluorescence: A Probe of Photosynthesis *In Vivo*. *Annual Review of Plant Biology* **59**, 89–113, <https://doi.org/10.1146/annurev.arplant.59.032607.092759> (2008).

Acknowledgements

We would like to recognise the work of John Srnka who collaborated on the design of the TECAN's LED lighting system and conducted all related programming and electrical work; Dr Nick Hamilton and James Lefevre for their input on the statistical analysis reported in the manuscript. We also gratefully acknowledge the support of the Australian Research Council (Linkage grant LP150101147), University of Queensland International Scholarship (UQI) and the Science and Industry Endowment Fund (John Stocker Postdoctoral Fellowship PF16-087).

Author Contributions

Jennifer Yarnold, Juliane Wolf and Ben Hankamer conceived and designed the experiments. Shwetha Sivakaminathan and Jennifer Yarnold performed the experiments. Shwetha Sivakaminathan, Jennifer Yarnold and Juliane Wolf analysed the data. Shwetha Sivakaminathan, Jennifer Yarnold and Juliane Wolf drafted the article. Ben Hankamer revised it critically and provided the funds and infrastructure for conducting the research at the Institute for Molecular Bioscience.

Additional Information

Supplementary information accompanies this paper at <https://doi.org/10.1038/s41598-018-29954-x>.

Competing Interests: The authors declare no competing interests.

Publisher's note: Springer Nature remains neutral with regard to jurisdictional claims in published maps and institutional affiliations.



Open Access This article is licensed under a Creative Commons Attribution 4.0 International License, which permits use, sharing, adaptation, distribution and reproduction in any medium or format, as long as you give appropriate credit to the original author(s) and the source, provide a link to the Creative Commons license, and indicate if changes were made. The images or other third party material in this article are included in the article's Creative Commons license, unless indicated otherwise in a credit line to the material. If material is not included in the article's Creative Commons license and your intended use is not permitted by statutory regulation or exceeds the permitted use, you will need to obtain permission directly from the copyright holder. To view a copy of this license, visit <http://creativecommons.org/licenses/by/4.0/>.

© The Author(s) 2018